Design and Preliminary Performance of the New Injection Shift Bump Power Supply at the J-PARC 3-GeV RCS

T. Takayanagi, N. Hayashi, M. Kinsho, T. Ueno, T. Togashi, K. Horino, and Y. Irie

***Abstract*—A new power supply for the injection shift bump magnet at the Japan Proton Accelerator Research Complex 3-GeV Rapid Cycling Synchrotron has been designed with the energy upgrading of the linear accelerator to 400 MeV. The power supply is required to output the maximum current of 32 kA, which is 1.6 times the present current. Moreover, peak current ripple noise should be less than $\pm 0.2\%$ of the setting current in a range from 10 kA to 32 kA output current. The insulated gate bipolar transistor chopping system in the present power supply produces the continuous current ripple noise due to the switching, which resonates with the load and excites a forced beam oscillation at about 96 kHz in the injection stage. So, the circuit structure of the new power supply has been changed from the insulated gate bipolar transistor chopping system to the pulse forming network system by switching capacitors. The whole power supply is comprised of 16 banks, each of which outputs 2 kA at 13.2 kV maximum. The first bank has been manufactured and the characteristics were evaluated in the factory. This paper summarizes the design and the preliminary experimental results of the new power supply.**

***Index Terms*—Insulated gate bipolar transistor (IGBT) and pulse forming network (PFN), Japan Proton Accelerator Research Complex (J-PARC), power supply, shift bump.**

I. Introduction

THE 3-GEV Rapid Cycling Synchrotron (RCS) [1], [2] of the Japan Proton Accelerator Research Complex (J-PARC) [3], [4] produces a high intensity beam for the 50-GeV Main Ring (MR) [4] and the Material and Life Science Experimental Facility (MLF) [4]. In the 1st stage, injection energy from the linear accelerator (LINAC) and the extraction energy are 181 MeV and 3 GeV, respectively. The design of the output power is 0.6 MW at the maximum [5], [6]. In the 2nd stage, the injection energy is upgraded to 400 MeV. The primary goal of the RCS is to output the 1 MW beam power. With the injection energy upgrade to 400 MeV, the power supply capacity of the injection shift bump (SB) magnet should be increased by 1.6 times [7], [8]. Furthermore, in the commissioning of the high-intensity beam test with the present SB power supply, which is the system of an insulated gate bipolar transistor (IGBT) chopping system, it was observed that the second harmonic component of 48 kHz ripple currents due to the IGBT switching resonates with the betatron tune at about 96 kHz [9]. Therefore, the new SB power supply has been designed for ripple-free operations, where the maximum output current is 32 kA and the circuit system comprises a pulse forming network system by switching capacitance [10]. The preliminary test has been performed and the measurements of the characteristic were evaluated.

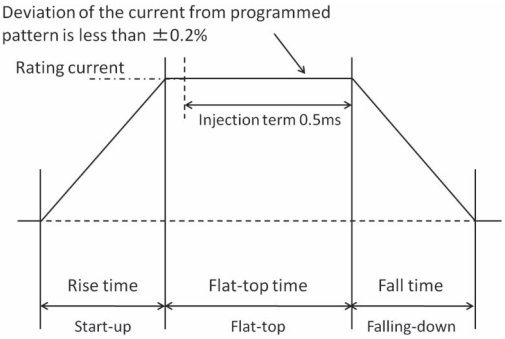

Fig. 1. Schematic view of the trapezoidal waveform pattern produced by the SB power supply.

II. Design and Performance of the Power Supply

A. Overview of the Injection SB Magnet System

The SB magnet produces a fixed main bump orbit to merge the injection beam from the LINAC into the circulating beam of the RCS [5], [6]. In the new SB power supply for 400 MeV injection beam energy, the performance of the power supply is required to be 1.6 times the output current and about twice the output voltage of the present one. The power supply produces the trapezoidal waveform pattern, as shown in Fig. 1. The flat-top of the trapezoidal waveform is used for fixing a beam orbit during the beam injection during 500 μs. The injection bump system performs the two functions: one is a source to produce the neutrons and muons at the MLF and the other is an injector to the MR. Each beam parameter is controlled by the output current of the shift bump magnet, which changes the excitation level by 25% at 25 Hz. Furthermore, the fall time of the waveform is arbitrary changed from 150 μs to 500 μs depending upon the temperature rise at the first charge-exchange foil [5].

B. Design of the New SB Power Supply Circuit

The rectifier of the new SB power supply has adopted the 24-pulse rectifier circuitry. This system has lower switching noise than the Pulse Width Modulation (PWM) rectifier used by the present SB power supply. The circuit system of the new

Manuscript received July 17, 2013; accepted December 23, 2013. Date of publication January 9, 2014; date of current version February 14, 2014.

T. Takayanagi, T. Ueno, K. Horino, T. Togashi, N. Hayashi, and M. Kinsho are with the Japan Atomic Energy Agency/Japan Proton Accelerator Research Complex (JAEA/JPARC), Naka-gun 319-1195, Japan (e-mail: tomohiro.takayanagi@j-parc.jp).

Y. Irie is with the KEK, Tsukuba 305-0801, Japan.

Digital Object Identifier 10.1109/TASC.2013.2297029

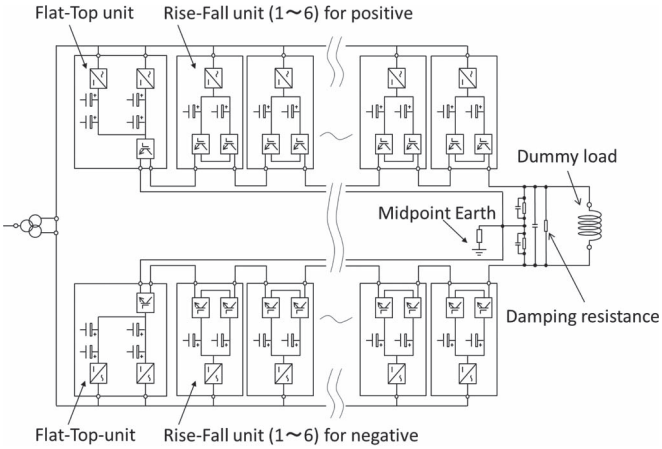

Fig. 2. Schematic view of the one bank, which is composed by 12 rise-fall units and the 2 flat-top units. All units are connected in series.

SB power supply has been designed as a pulse forming network (PFN) switching system. The PFN system is comprised of many capacitor banks, and utilizes a commutation strategy using the electrical charge and discharge of the capacitor. The main circuit of the new power supply is comprised of 16 banks in parallel. One bank produces the maximum current of 2 kA and the maximum output voltage is 13.2 kV. Each bank is connected in parallel and the maximum current is 32 kA. The schematic view of the one bank is shown in Fig. 2. One bank is comprised of the 12 rise-fall units and the 2 flat-top units, which are connected in series. The rise-fall unit has a function of the starting-up and the falling-down of the trapezoidal waveform. The flat-top unit has a function to maintain the flatness of the trapezoidal waveform. The circuit is divided on the basis of the midpoint earth. By the midpoint earth, the voltage across a magnet terminal and ground can be reduced by half ($\pm$6.6 kV).

In order to alter the output waveform, the charging voltage of the main capacitor in each unit is changed. However, since a rise and a fall times are the same, which varies from 150 μs to 500 μs, the starting-up and the falling-down process are controlled by the same unit. As for the flat-top time, it is fixed in 650 μs due to the charging capability of the DC power supply. The flat-top unit has two charging circuits in one unit: one corresponds to the beam for the MLF and the other for the MR.

C. Rise-Fall Unit

The schematic view of the basic circuit of the rise-fall unit is shown in Fig. 3. The main capacitor C is an aluminum electrolytic capacitor, which is newly developed for the new SB power supply to realize higher capacitance in a small volume. The size of the capacitor is 90 mm in diameter and 250 mm in height, having a characteristic of 24 mF with 350 V rating. This enables the compact configuration of the power supply. The capacitor is charged by the DC power supply (1.5 kW/ 600 V). Each operation mode consists of powering, regeneration and free-wheeling modes (Fig. 3). The waveform pattern of the output current at the trapezoidal shape has been produced by 4 switchings, which are located at the start of start-up mode, flat-top mode and falling-down mode, and at the switch off, as shown in Figs. 1 and 3.

The design of the snubber circuit at the rise-fall unit has been optimized. The measurement results of the output current and

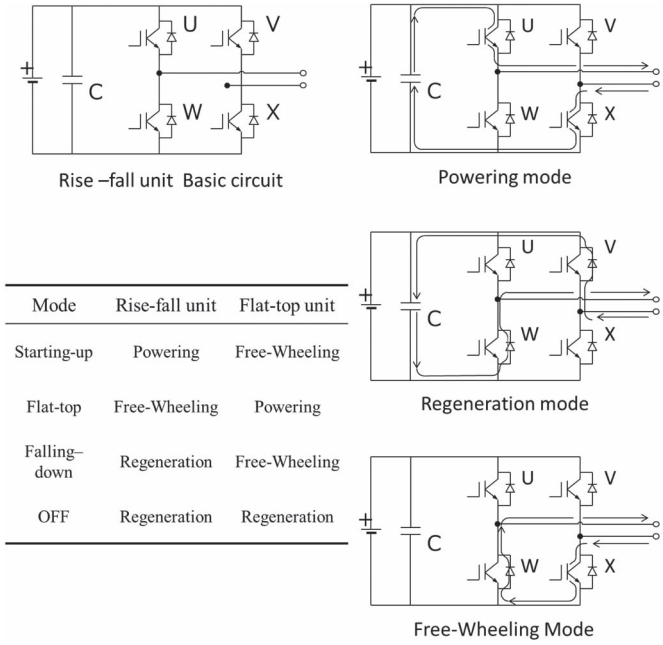

Mode	Rise-fall unit	Flat-top unit
Starting-up	Powering	Free-Wheeling
Flat-top	Free-Wheeling	Powering
Falling–down	Regeneration	Free-Wheeling
OFF	Regeneration	Regeneration

Fig. 3. Schematic view of the basic circuit of the rise-fall unit and current flow in each operation mode.

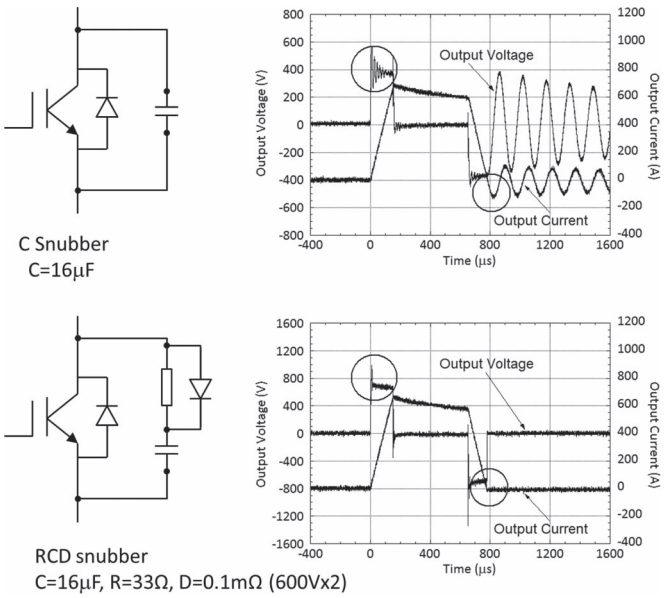

Fig. 4. Measurement result of the output current and output voltage.

voltage are shown in Fig. 4. Large ringings of both the output voltage and the current are seen for the C snubber circuit. The ringing frequency is about 60 kHz. The resonance source is the C (16 μF) of the snubber and the load inductance. In the case of the RCD snubber, where the resistance (R) is 33 Ω, capacitance (C) 16 μF, and diode (D) about 0.1 mΩ, the ringing was well suppressed.

The impedance and the output waveform of the current and the voltage at the unit were measured. For comparison, the circuit of the rise-fall unit has been simulated by using simulation code, Micro-cap. The results are shown in Fig. 5. Both the internal impedance of one unit measured looking into the output terminals and the output waveforms of the current and the voltage agree well with the simulation.

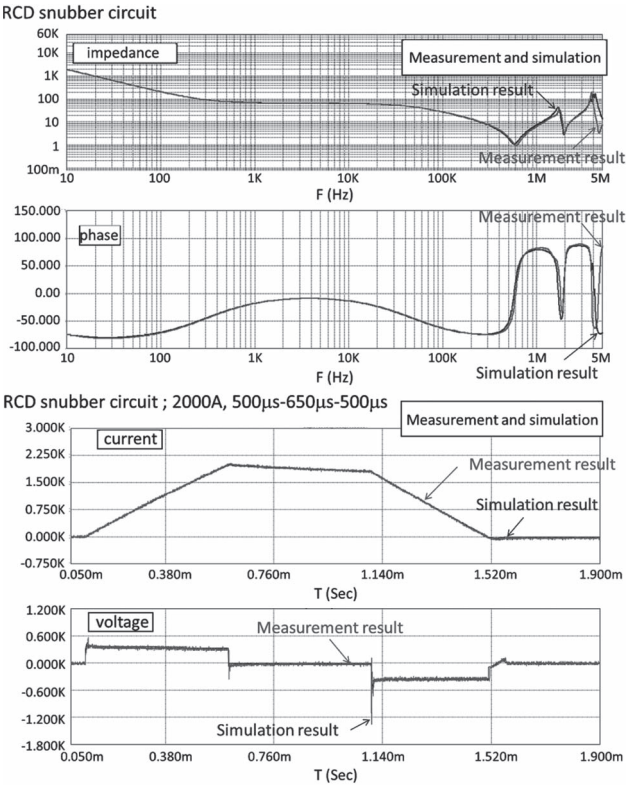

Fig. 5. Comparison between measurements and simulations of the internal impedance, output current, and voltage.

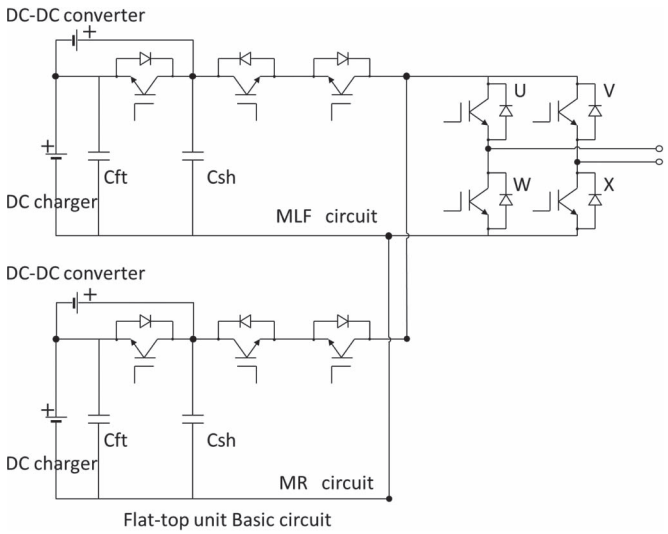

Fig. 6. Schematic view of the basic circuit of the flat-top unit.

D. Flat-Top Unit

The schematic view of the basic circuit of the flat-top unit is shown in Fig. 6. There are two main capacitors. One is an aluminum electrolytic capacitor (C_{ft}) and another is a film capacitor (C_{sh}). C_{ft} is the same capacitor (24 mF, 350 V) as in the rise-fall unit, which is composed by 8 capacitors. The DC power supply for the capacitor charging is 300 V/40 A. By changing the connection of capacitor elements, it is possible to realize the main capacitance of 48 mF, 96 mF, 120 mF, 144 mF, 168 mF, and 192 mF, if it is necessary to fine control the waveform. The film capacitor is 2 mF. The film capacitor is charged by a DC-DC converter (450 V/20 A). The snubber

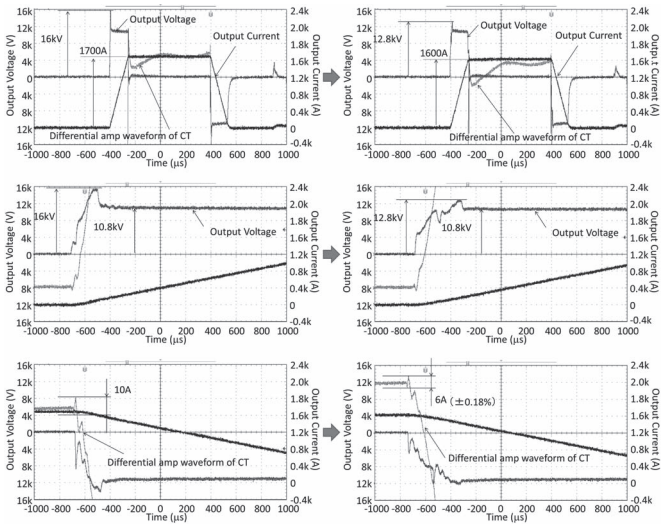

Fig. 7. Measurement result of the output current and the voltage before and after adjusting the timing gate. Timing gate of rise-fall unit (two pairs: 1, 3, 5, 6 and 2, 4) shifts 10 μs.

circuit of the flat-top unit adopts the RC snubber to suppress the ringing. The circuit simulation has also been performed in the same way as the rise-fall unit. The simulation results agreed well with the measurement results.

III. Preliminary Test Result of One Bank

The output waveforms for one bank have been measured.

A. Reduction of the Ringing at the Waveform

In the current and voltage waveforms, large ringing was confirmed. In case of the fast rise and fall time with 150 μs, the overshoot peak voltage reached 16 kV. In order to reduce the peak voltage, the gate timing of the operation start of the rise-fall unit was shifted in pairs for each unit in Fig. 2. One group comprises pairs of 1, 3, 5 or 6 in the positive and negative sides and the other group comprises pairs of 2 and 4. There is a difference in the gate timing of 10 μs between the groups. After adjustment, the peak voltage is decreased to 12.8 kV. Furthermore, the current ripple is decreased from 10 A to 6 A, which is $\pm 0.18\%$. This result satisfies the requirement of the new bump power supply. These results are shown in Fig. 7.

B. Deviation Due to Change of Operation Mode

The change of the output current to satisfy the beam parameter for the MLF and the MR modes has been performed at 25 Hz. In the timing sequence, continuous 20 cycles for the MLF mode are followed by 5 cycles for the MR mode. The rise-fall units of Nos.1–4 and No.6 are used for the MLF, and Nos.1–4 and No.5 units are for the MR. As for the flat-top unit, the charging circuit is internally switched according to the operation mode as described previously.

The measurement result, which is the history during 10 seconds, is shown in Fig. 8. Each setting parameter is shown in Table I. The snubber circuits of the rise-fall unit and the flat-top unit are type of RCD and RC snubbers, respectively. The ringing of the flat-top is a noise due to switching of a rectifier for the DC power supply at 12 kHz. The current deviations at the flat-top period during 500 μs become less than $\pm 0.12\%$

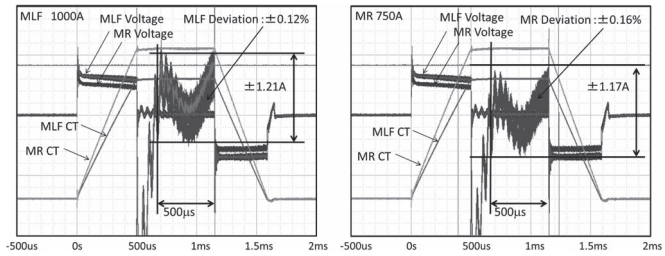

Fig. 8. Output current deviation during 10 s at 25 Hz. Continuous 20 cycles for the MLF mode are followed by 5 cycles for the MR mode.

TABLE I
SETTING PARAMETER OF EACH UNIT

Rise-fall unit No.	MLF(1000A)	MR(750A)
P6/N6	296.0V	Not Used
P5/N5	Not Used	125.0V
P4/N4	152.7V	152.7V
P3/N3	152.7V	152.7V
P2/N2	152.7V	152.7V
P1/N1	152.7V	152.7V

Flat-top/DD	MLF(1000A)	MR(750A)
DC power supply	85V	73.5V
DD converter	139V	118.1V

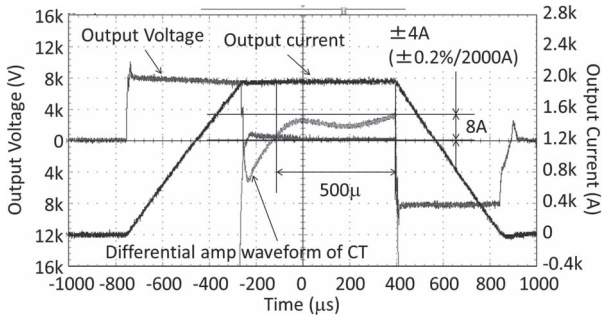

Fig. 9. Measurement result of the output waveform of the current and voltage. The setting parameter of the rise and fall time is 500 μs.

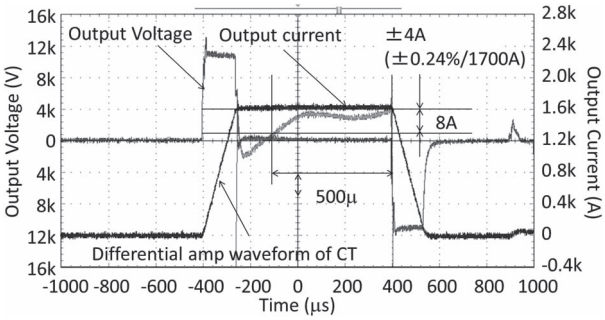

Fig. 10. Measurement result of the output waveform of the current and voltage. The setting parameter of the rise and fall time is 150 μs.

and ±0.16% for the MLF and MR modes, respectively. These results satisfy the specifications.

C. Flatness of the Flat-Top With Different Rise and Fall Times

The flatness accuracy of the flat-top period at rating output of one bank was confirmed at 1 Hz. The measurement results of each output waveform are shown in Figs. 9 and 10. The rise and fall times are 500 μs and 150 μs, and the output currents are 2000 A and 1700 A, respectively. The snubber circuits of the rise-fall unit and flat-top unit are of RCD and RC snubbers, respectively. Furthermore, the damping resistor of 100 Ω is installed across the output terminal of the power supply so that higher frequency oscillation of 500 kHz could be dumped. The result with 500 μs fall time satisfies the requirement. However, in the case of the 150 μs, further adjustment is required to reduce the deviations. At flat-top start point, the decay time constant of the transient peak is longer than 500 μs because of the inductance of the load. Fine adjustments of the output voltages of the DC power supply and DC-DC converter have been continued to lower the transient peak, will keeping the flat-top current at the required level.

IV. CONCLUSION

The power supply of the new shift bump magnet with the PFN switching capacitor method has been designed and preliminary tests were performed. Operation with 500 μs fall time satisfies the specifications. However, in the case of the 150 μs fall time, further adjustment is required to reduce the deviations. Manufacturing the remaining banks and investigations of higher output current accuracy with multi-bank operations are in progress.

ACKNOWLEDGMENT

One of the authors (T. Takayanagi) is grateful to K. Okabe (J-PARC) for his calculation support and K. Toda (NICHICON KUSATSU CORPORATION) for his continuous support.

REFERENCES

[1] N. Hayahsi, H. Harada, K. Horino, H. Hotchi, J. Kamiya, M. Kinsho, P. K. Saha, Y. Shobuda, T. Takayanagi, N. Tani, T. Togashi, T. Ueno, M. Watanabe, Y. Watanabe, K. Yamamoto, M. Yamamoto, Y. Yamazaki, M. Yoshimoto, Y. Irie, and T. Toyama, "Progress of injection energy upgrading project for J-PARC RCS," in *Proc. IPAC*, 2013, pp. 3833–3835, THPWO032.

[2] M. Kinsho, "Status and progress of the J-PARC 3 GeV RCS," in *Proc. IPAC*, 2013, pp. 3848–3850, THPWO037.

[3] Y. Yamazaki, "Accelerator technical design report for high-intensity proton accelerator facility project," J-PARC, Tokai, Japan, KEK-Rep. 2002-13; JAERI-Tech 2003-044, 2003.

[4] Website of the J-PARC Accelerator. [Online]. Available: http://j-parc.jp/Acc/en/index.html

[5] T. Takayanagi, J. Kamiya, M. Watanabe, Y. Yamazaki, Y. Irie, J. Kishiro, I. Sakai, and T. Kawakubo, "Design of the injection bump system of the 3-GeV RCS in J-PARC," *IEEE Trans. Appl. Supercond.*, vol. 16, no. 2, pp. 1358–1361, Jun. 2006.

[6] T. Takayanagi, J. Kamiya, M. Watanabe, T. Ueno, Y. Yamazaki, Y. Irie, J. Kishiro, I. Sakai, T. Kawakubo, S. Tounosu, Y. Chida, M. Watanabe, and T. Watanuki, "Design of the shift bump magnets for the beam injection of the 3-GeV RCS in J-PARC," *IEEE Trans. Appl. Supercond.*, vol. 16, no. 2, pp. 1366–1369, Jun. 2006.

[7] T. Takayanagi, N. Hayashi, T. Ueno, T. Togashi, and Y. Irie, "Simulation model for design of a new power supply," *IEEE Trans. Appl. Supercond.*, vol. 22, no. 2, p. 5400704, Jun. 2012.

[8] T. Takayanagi, N. Hayashi, T. Ueno, T. Togashi, N. Tani, M. Kinsho, and K. Toda, "New power supply of the injection bump magnet for upgrading the injection energy in the J-PARC 3-GeV RCS," in *Proc. IPAC*, 2012, pp. 3226–3628, THPPD051.

[9] H. Hotchi, M. Kinsho, K. Hasegawa, N. Hayashi, Y. Hikichi, S. Hiroki, J. Kamiya, K. Kanazawa, M. Kawase, F. Noda, M. Nomura, N. Ogiwara, R. Saeki, P. K. Saha, A. Schnase, Y. Shobuda, T. Shimada, K. Suganuma, H. Suzuki, H. Takahashi, T. Takayanagi, O. Takeda, F. Tamura, N. Tani, T. Togashi, T. Ueno, M. Watanabe, Y. Watanabe, K. Yamamoto, M. Yamamoto, Y. Yamazaki, H. Yoshikawa, and M. Yoshimoto, "Beam commissioning of the 3-GeV rapid cycling synchrotron of the Japan proton accelerator research complex," *Phys. Rev. ST—Accel. Beams*, vol. 12, no. 4, pp. 040402-1–040402-22, Apr. 2009.

[10] T. Takayanagi, N. Hayashi, K. Horino, M. Kinsho, T. Togashi, T. Ueno, Y. Watanabe, and Y. Irie, "Power supply of the pulse steering magnet for changing the painting area between the MLF and the MR at J-PARC 3 GEV RCS," in *Proc. IPAC*, 2013, pp. 681–683, MOPWA008.